RESEARCH ARTICLE

WILEY

DTM resolution controls the accuracy of estimating surface runoff indicators in flat, lowland landscapes

Peter Schaap[1] | Ype van der Velde[2] | Perry de Louw[1,3] |
Harm Bartholomeus[1]

[1]Department of Environmental Sciences, Wageningen University, Wageningen, The Netherlands

[2]Department of Earth Sciences, Vrije Universiteit Amsterdam, Amsterdam, The Netherlands

[3]Department of Soil and Groundwater, Deltares, Utrecht, The Netherlands

Correspondence
Peter Schaap, Droevendaalsesteeg 3, 6708 PB Wageningen, The Netherlands.
Email: peter1.schaap@wur.nl

Abstract

Surface runoff plays an important role in contaminant transport, nutrient loss, soil erosion and peak discharges in streams and rivers. Because it is the result of a variety of complex hydrological processes, estimating surface runoff using physically based hydrological models is challenging. Upscaling of physical soil properties is necessary to cope with the limits of computational power in surface runoff modelling. In flat landscapes, the (micro)topographic surface controls the onset and progression of surface runoff on saturated soils during rain events. Therefore, its proper representation is crucial when attempting to model and predict surface runoff. In this study, the influence of microtopography (centimetre scale) on estimations of maximum depression storage (MDS), random roughness (RR) and the connectivity threshold (CT) is explored. These properties are selected because they often serve as surface runoff indicators in hydrological modelling. To characterize microtopography, a terrestrial laser scanner (TLS) is used to generate a digital terrain model (DTM) of the study site with a horizontal spatial resolution of 5 cm. MDS, RR and CT are then calculated and compared to the values generated from the publicly available Dutch national DTM dataset with a resolution of 50 cm. Our results show considerable differences in MDS, RR and CT when calculated for the different input resolution datasets. Using DTMs that do not sufficiently capture microtopography leads to underestimation of MDS and RR, and to overestimation of CT. Our findings indicate that surface runoff indicators, and thereby the surface runoff response of a saturated surface to rainfall events, are defined at scales smaller than the scales of typically available DTMs. Understanding surface runoff through modelling studies therefore requires a framework that accounts for this lack of information arising from using coarser resolution DTMs. We demonstrate a linear relationship between MDS values generated from the different resolution DTMs. This opens the possibility of using empirical scaling relationships between high- and lower-resolution DTMs to account for

microtopography. Repetition of our measurements on similar surfaces would contribute to establishing such empirical scaling relationships. Our results should be seen as indicative of flat landscapes and surfaces where centimetre scale microtopography is relevant.

1 | INTRODUCTION

Surface runoff is an important pathway for nutrient losses (e.g., Burwell et al., 1975; Haygarth et al., 2005; K.A. Smith et al., 2001; R. Smith et al., 2015) and contaminant transport (e.g., Chrétien et al., 2017; Coyne et al., 1995; Peyton et al., 2016; Rakonjac et al., 2022) from agricultural fields to surface waters. In this capacity, surface runoff has been linked to eutrophication and algal blooms (Dolph et al., 2019; Sharpley et al., 1994; Wurtsbaugh et al., 2019), loss of biodiversity (Dudgeon, 2019; Leip et al., 2015) and drinking water pollution (Dąbrowska et al., 2018; Gilliom, 2007; Kool et al., 2023). As surface runoff also leads to soil erosion and contributes to peak discharges in streams and rivers, there is a need for scientists and water managers to assess its occurrence, magnitude, and relative contribution to nutrient and contaminant transport (Massop et al., 2017; van der Velde et al., 2010; Worm et al., 2019). In the context of European legislation like the Water Framework Directive, knowledge of the relative contribution of surface runoff to the deterioration of surface waters can prove vital in achieving the proposed environmental quality standards (EC, 2000; Heathwaite & Dils, 2000). Furthermore, with climate change projections indicating an increase in the frequency of extreme weather events (Coumou & Rahmstorf, 2012), studies on surface runoff will become increasingly pertinent.

Measuring surface runoff in field conditions can be time consuming, expensive, and often requires intensive maintenance (De Louw et al., 2015; van der Velde et al., 2010). Case studies in scientific literature are scarce and if present, conducted in lab-context or on small plots covering up to several square meters (e.g., Chu et al., 2012; Gomi et al., 2008; Joel et al., 2002; Soultani et al., 1993). Consequently, there is an important role for modelling studies in gaining a better understanding of this hydrologic phenomenon and in translating insights from smaller scales to scales relevant for water management (catchments >5 km^2). Surface runoff is influenced by various factors, both natural and human-induced, including topography, meteorology, climate, local micro- and macro-biota, antecedent soil moisture, soil characteristics, vegetation cover and changes in land use and land cover. Because surface runoff is the result of a variety of complex and highly non-linear hydrological processes and interactions, physically based modelling approaches are prone to overparameterization, numerical instability or excessive computation times (Beven, 1989; Frei et al., 2010; Zhang & Cundy, 1989). This is particularly true when one considers the scale of the relevant processes involved.

Microtopography on the centimetre scale plays an important role in the onset and progression of surface runoff (Dunne et al., 1991; Frei & Fleckenstein, 2014). Especially in flat landscapes such as lowlands and river deltas, where horizontal flow velocity is low and surface runoff is less influenced by erosion and preferential flow paths, microtopography controls the responsiveness of a saturated surface to rain events (Antoine et al., 2009; Appels et al., 2016). Woolhiser (1996) even argued that a reasonable estimation of surface runoff cannot be made without proper measurements of microtopography. In physically based hydrological models, it is not feasible to perform calculations with grid cells on this level of detail (Frei & Fleckenstein, 2014). Therefore, microtopography is often parameterized using subgrid concepts describing surface storage, surface roughness or surface connectivity. Because of the runoff controlling nature of microtopography, these properties can be regarded as surface runoff indicators.

Characterizing microtopography as a storage component provides an intuitive parameter, the maximum depression storage (MDS), which is widely applied in hydrological models with various degrees of complexity (e.g., Aquanty, 2015; Beven & Kirkby, 1979; DHI, 2023; Kroes et al., 2017; Markstrom et al., 2015; Neitsch et al., 2011; Panday & Huyakorn, 2004). MDS describes the maximum volume of water that can be stored on the surface and often functions as a threshold-type parameter that must be filled before surface runoff can occur. It can be estimated directly from elevation data using filling algorithms, as a lumped parameter through model calibration or by empirical relationships with surface roughness indices. As this study is focussed on the representation of topography, the method utilizing model calibration is not considered further here. The disadvantage of using filling algorithms in estimating MDS is that grid data that can capture all relevant topographic features is often not available. Roughness indices offer an alternative method of calculating MDS that accounts for microtopography (Chu et al., 2012). Kamphorst et al. (2000) provide an overview of different roughness indices and how they relate to MDS and found that random roughness (RR), which is the standard deviation of a surface corrected for general slope, is most suited for estimation of MDS. The advantage of deriving MDS from RR is that RR can be calculated directly from spot measurements of elevation (e.g., observed with laser techniques or manual pin measurements), while for filling-algorithm-based estimates of MDS these spot measurements need to be interpolated into a spatial grid, losing important fine-scale information (e.g., Thomas et al., 2017; Yang & Chu, 2013). Antoine et al. (2009) argued that fields with similar geostatistical properties (i.e., variogram) can have different rainfall-runoff responses, depending on

the connectivity of microchannels and gullies in the landscape. Peñuela et al. (2013) further developed this idea by creating a parameter, the connectivity threshold (CT, see Section 2), that indicates at which depression storage a field starts to produce runoff. This typically is far before the full MDS is reached and depends on the connectivity of depressions to the outflow boundary. This concept of hydrologic connectivity in combination with MDS has potential to improve runoff description in hydrologic models (Peñuela et al., 2015).

Estimating MDS, RR and CT requires a proper representation of the hydrologic surface. The resolution of publicly available digital terrain models (DTMs) is often not sufficient for capturing microtopography on the centimetre scale. Furthermore, interpolation in the pre-processing phase of the DTM product may lead to smoothing of the elevation profile and alter its geostatistical properties (Desmet, 1997; Li et al., 2020). As these DTMs are widely used in terrain analysis and hydrologic modelling, it is important to consider the influence of DTM resolution and construction methods on the representability of the dataset. Recent developments in data processing capacity and measurement technology, like terrestrial- and airborne-laser scanning, have made it possible to construct a surface in great detail (Harpold et al., 2015; Telling et al., 2017). Terrestrial laser scanners have been used in numerous studies to generate high resolution DTMs and evaluate the effects of small-scale topography in earth science research (e.g., Barneveld et al., 2019; Fan & Atkinson, 2018; Jan et al., 2018; Li et al., 2020).

The research objectives of this study are to assess the influence of DTM resolution on estimating surface runoff indicators and to explore how we may account for small scale microtopography when only relatively coarse, public DTMs are available. Addressing these objectives will increase our understanding of the topographic properties governing surface runoff in flat landscapes, shed light on the level of detail required to estimate surface runoff through modelling studies, and improve the interpretation of the outcomes of modelling studies utilizing publicly available DTMs.

A case study is presented in which a terrestrial laser scanner (TLS) is used to generate a DTM with a horizontal spatial resolution (hereafter referred to as: resolution) of 5 cm. The 5 cm-DTM is then used to determine MDS, RR and the CT. These properties are then compared with a similar set of values calculated for a different input DTM with a lower resolution of 50 cm, AHN3, which is the publicly available Dutch national DTM (see: https://pdok.nl/). This case study highlights the significance of microtopography in characterizing a surface used to estimate surface runoff indicators and explores empirical relationships between DTM-derived parameters from high- and lower-resolution datasets. Such relationships will improve the representation of microtopography in surface runoff studies.

2 | METHODS

2.1 | Site description

The study site, located in the Twente region in the eastern part of The Netherlands, is a low slope (average slope <1%) 1.4 ha permanent
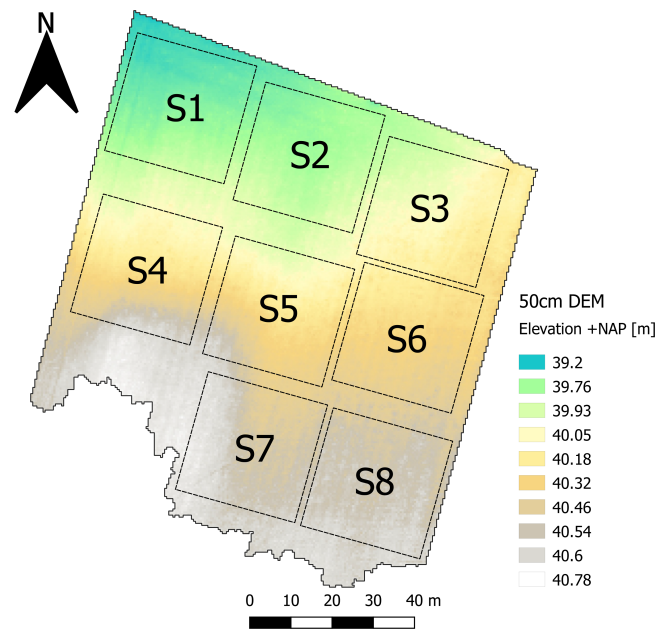
FIGURE 1 50 cm-DTM of the study site with surface samples S1–S8.

grassland used for grazing by dairy cows (Figures 1 and 2). The field has been used in this way for over a decade and apart from rotational grazing, agricultural activities are limited to mowing (twice a year) and fertilizer injections (twice a year). The topsoil (0–20 cm below the surface) consists of moderately fine sand with organic matter (approximately 5%) and traces of silt and loam (both approximately 10%; see: https://www.dinoloket.nl). The studied sub-catchment within the field is bordered by a ditch in the north, the hydrological divide in the south, a ridge in the west and continuing grassland in the east. Around 25% of the land surface of The Netherlands is permanent grassland and it is considered an important source of nutrient and contaminant transport (de Vries et al., 2021; Rakonjac et al., 2023).

2.2 | Topographic data

The study site is discretized into regular grid digital terrain models (DTMs) in two horizontal spatial resolutions: 5 and 50 cm. The resolutions are chosen to distinguish between micro- and meso-topographic surface features within the context of flat landscapes. The 5 cm-DTM can capture microtopographic structures, that is, tussocks and the spaces in between that are characteristic for lowland cattle pastures (Figure 2b). The choice for a 5 cm-DTM is supported by the works of Kamphorst et al. (2000) and Habtezion et al. (2016), who found no changes in storage and topographic properties at grid sizes below 40 mm (test range 2–40 mm) and 10 cm (test range 2–80 cm) respectively. In contrast, the 50 cm-DTM is too coarse to capture the micro-topographic features characteristic for our study site. By using both resolutions, this study aims to evaluate how microtopography and input DTM resolution influence estimates of the surface runoff indicators selected in this study. Another reason for selecting the

FIGURE 2 (a) Wide view photograph of the study site, a typical Dutch cattle pasture, taken in the summer of 2023. (b) Close up photograph, taken in a wet period in the winter of 2024, showing water stored in surface depressions between tussocks. Some of the smaller puddles have merged, increasing the hydrologic connectivity of the surface.

50 cm-DTM is because it has national coverage (The Netherlands) and therefore offers potential scaling and application opportunities.

The 5 cm-DTM was obtained through a LiDAR survey in November 2021, using a Riegl® VZ-400 terrestrial laser scanner (TLS) mounted on an extendable tripod of approximately 3.5 m in height. The scanner was placed in vertical position, scanning 360° in horizontal and between 130° and 30° relative to nadir in vertical direction (Figure 3). This means that the ground surface close to the scanner was not sampled directly, but from an adjacent scan position. This resulted in slightly lower point densities directly around the locations where the scanner was placed. The angular resolution of the scanner was set to 0.04°, resulting in point densities between 10 000 and 100 000 points/m². The different scans were co-registered using 5 cm-diameter retro-reflective tubes, placed between the scan positions. Absolute geo-referencing was done based on the add-on GPS receiver and the point clouds were levelled based on the inclination sensors of the instrument. Surface points were extracted using the lasground_new module of the LAStools software package (see: https://rapidlasso.com/lastools/), which has demonstrated good results in earlier studies (Moudrý et al., 2020). It applies progressive triangulated irregular network (TIN) densification. The module first extracts the lowest points for each cell within a user defined grid, which we set at 25 cm (the size of the largest surface feature: a tussock), from which it builds an initial TIN. This is

then densified by iterating over the points in the point cloud, in which ground- (progressively added to the TIN) and non-ground points are classified based on distance and angle to the TIN plane and nodes. As we worked with a 25 cm initial grid on a relatively flat surface, we removed spikes above 15 cm from the initial TIN plane, as such steps were considered non-ground (vegetation) points. The algorithm allows for slight 'bulging' (we used the default 2.5 cm: one tenth of the initial grid size) of the calculated surface. The result of the lasground_new module is a fine resolution TIN containing all classified ground points. Next, the blast2dem module applies inverse distance weighting (IDW) to transform the TIN to a 5 cm regular grid (see: https://rapidlasso.com/blast/blast2dem/). The 50 cm-DTM used in this study is the open source AHN3 dataset, which covers all of The Netherlands (see: https://app.pdok.nl/viewer). The part of the dataset covering the study site was generated in 2012 using airborne laser imagery with a point cloud density of 10–14 points/m². The point clouds were classified into surface and non-surface points (partly automated, partly by hand) and transformed to the 50 cm-DTM using squared inverse distance weighting to estimate the elevation at the centre of the grid cell (see: https://ahn.nl/ahn-the-makin-of). To allow for comparison of the DTM-derived surface runoff indicators within the study site, random rectangular surface samples were selected by hand with dimensions 30 × 30 m (Figure 1). The size of the samples was chosen following
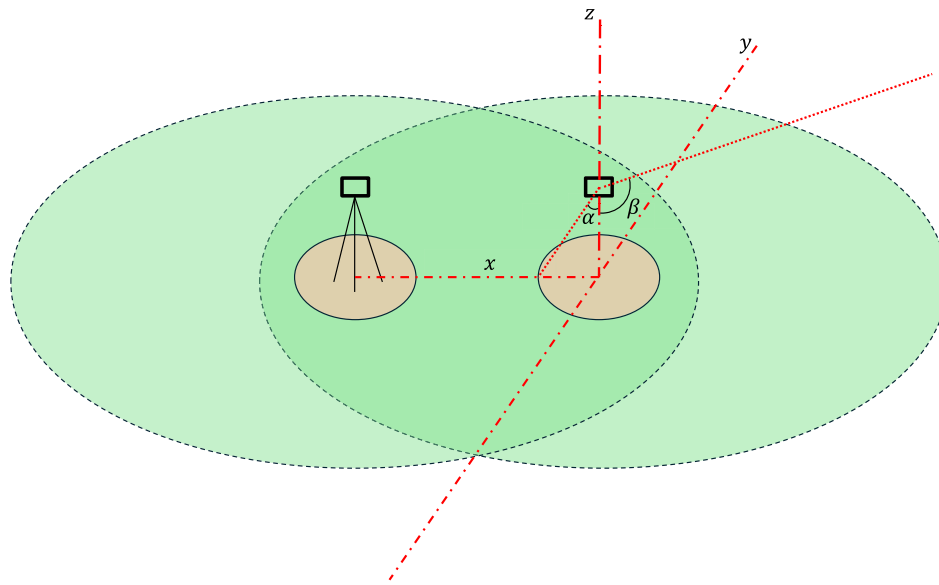
FIGURE 3 Depiction of the TLS measurement procedure. Red circles portrait the 'blind zone' right below the TLS (black rectangle), resulting from the 30° angle α with respect to nadir (vertical line z). The blind spot is measured from an adjacent position, leading to differences in point densities at different locations on our study site. In our case study, the point densities varied from 10 000 to 100 000 points per square meter. The study site was measured from 20 different scanning positions throughout the field, at approximately 20–30 m (horizontal line x) from each other in a grid-wise movement (5 rows in the west–east direction, 4 columns in the north–south direction). The 130° angle β represents the maximum angle at which the TLS scans its surroundings. The actual 'line of sight' of the TLS is obtained by subtracting angle α (30°) from angle β (130°) and results in a viewing angle of 100°. This wide angle allows the TLS to, apart from its blind zone, scan the complete study site from every scanning position (illustrated by horizontal line y).

Appels et al. (2011), who proposed a maximum semivariogram range/field length ratio of 0.1 for a representative sample of a randomly distributed surface. The average semivariogram range of the field samples is approximately 2 m, yielding a range/field length ratio of 0.067.

2.3 | Surface runoff indicators

The three surface runoff indicators used in this study, maximum depression storage (MDS), random roughness (RR) and connectivity threshold (CT) are chosen based on their popularity in scientific literature and on their relevancy in hydrologic modelling (e.g., Chu et al., 2010; Kamphorst et al., 2000; Martin et al., 2008; Peñuela et al., 2015; Yang & Chu, 2013).

2.3.1 | Maximum depression storage

MDS, also called surface depression storage or depression storage capacity, is the maximum volume of water that can be stored in depressions on a surface (Amoah et al., 2013). It is a ubiquitous concept, often functioning as a threshold-type parameter in surface runoff-related modelling. A depression within a DTM can be mathematically defined based on the elevation values of the grid cells surrounding a given centre cell. If the centre cell has a lower elevation than its neighbouring cells, it is considered a surface depression. The

sum of the volumes of all surface depressions in a DTM is considered the MDS, and is usually normalized over the area to be expressed in millimetres. As surface depressions often consist of clusters of grid cells, the most common way of calculating MDS is by iterating over the grid cells in a DTM, gradually 'filling' the depressions until none remain. In this study, we apply the SAGA GIS Wang & Liu filling algorithm to derive MDS directly from the DTMs (Wang & Liu, 2006). The algorithm creates a spatially distributed map of surface depressions. MDS is obtained by filling up surface depressions in order of a priority queue that starts with the lowest outflow boundary grid cell and expands every iteration. The outflow boundaries are located at all sides of the analysed surface. The algorithm progressively connects the regular grid to the outflow boundary, applying a least-cost scheme that selects the lowest elevation of all eight neighbouring cells to generate optimal flow paths. In the final stage the complete surface is connected to an outflow boundary and MDS can be determined. It is considered efficient and accurate and is widely adopted in scientific literature (e.g., Jensen et al., 2017; Kopecký et al., 2021; Niittynen et al., 2018).

2.3.2 | Random roughness

The concept of random roughness (RR), a measure of the elevational variability of a surface, is a popular way of statistically parameterizing topography in hydrology (e.g., Cremers et al., 1996; Hansen et al., 1999; Kamphorst et al., 2000; Moriasi et al., 2012; Mwendera &

Feyen, 1992; Onstad, 1984). It is usually derived from high resolution (mm-cm scale) pin-meter measurements and therefore able to account for microtopography. Its calculation however is subject to discussion as authors disagree on how to correct for slope and tillage, whether to use standard deviation or standard error, and whether to use log transformation in generating RR (Kamphorst et al., 2000). In this study, we follow the definition of Currence and Lovely (1970) and Kamphorst et al. (2000), who define RR as the standard deviation of elevation points in a transect of a DTM after correcting for slope. They argued against the use of standard error, as it would be directly related to the number of elevation data points. Furthermore, they did not perform log-transformation as RR is more sensitive to changes in roughness without it. Instead of using a transect, we use all elevation points in the DTM to generate RR to account for roughness in both x- and y-directions. Kamphorst et al. (2000) correct for slope using a linear trend plane, which is reasonable considering the small areas of their field plots, which range from 0.2 to 3.5 m^2. As this method may lead to outliers in the residuals and corresponding elevation points due to heterogeneity in the sloping surface, we chose to detrend the study site using SAGA's simple filter functionality in QGIS (see: https://sourceforge.net/p/saga-gis/wiki/grid_filter_0/). This module calculates the average value within a search radius for every point in a DTM and provides a straightforward approach for correcting a surface for general slope (Cavalli & Marchi, 2008). By making each calculated elevation grid cell in the trend surface a function of its neighbouring cells instead of one linear trend plane, we can account for heterogeneity in the sloping surface. The search radius of the moving average will affect the resulting detrended surface. The choice of this radius is subjective and depends on the purpose of the study and nature of the relevant topographic features (Trevisani et al., 2012). To evaluate the effect of search radius, the algorithm is repeated for search radii of 25, 50, 100, 150, 200, 250, 300, 350, 400, 450, and 500 cm. RR is then retrieved by taking the standard deviation of the residuals after subtracting the filtered DTM from the original DTM. The concept of RR is commonly employed in calculating MDS through empirical formulas utilizing RR and general slope as independent variables. To evaluate the impact of DTM resolution on RR-derived MDS estimates, we selected a range of popular empirical formulas (see Table 1; similar to Abd Elbasit et al., 2020) from scientific literature (Hansen et al., 1999; Kamphorst et al., 2000; Mwendera & Feyen, 1992; Onstad, 1984).

TABLE 1 Adapted from Abd Elbasit et al. (2020): the four empirical formulas using the concept of RR to calculate MDS.

Empirical formula	Reference
$MDS = 0.112 \cdot RR + 0.031 \cdot RR^2 - 0.012 \cdot RR \cdot S$	Onstad (1984)
$MDS = 0.294 \cdot RR + 0.036 \cdot RR^2 - 0.01 \cdot RR \cdot S$	Mwendera and Feyen (1992)
$MDS = 0.369 \cdot RR - 3.76 \cdot RR \cdot S + 11.1 \cdot RR \cdot S^2$	Hansen et al. (1999)
$MDS = 0.234 \cdot RR + 0.01 \cdot RR^2 + 0.012 \cdot RR \cdot S$	Kamphorst et al. (2000)

The use of such empirical formulas in hydrological models like the soil erosion model LISEM (De Roo et al., 1996) implies a level of generalizability. We included them to our analysis to explore their applicability beyond the data from which they were developed, and to publicly available DTMs such as the 50 cm-DTM used in this case study.

2.3.3 | Connectivity threshold

To assess the influence of microtopography on hydrologic connectivity, we follow the work of Darboux et al. (2002) and Antoine et al. (2009). These authors found that traditional indicators used to quantify spatial variability of surfaces, such as semivariograms and relative bivariate entropy are not able to distinguish between different landscape configurations with similar geostatistical properties. Antoine et al. (2009) developed a methodology that can capture the runoff dynamics of these different topographies, utilizing a fill-and-spill algorithm to generate a relative surface connection function (RSCf). The fill-and-spill model deposits a volume of water on a DTM per timestep and redistributes this water based on surface elevation and under the assumption of instantaneous water transfer. Surface depressions become ponds, which can merge into larger ponds until they reach the outflow boundary and become surface runoff. Plotting depression storage (m^3) (x-axis) against the ratio surface connected to the outflow boundary/total surface (−) (y-axis) yields the RSCf. To allow for comparison of different surfaces independent of surface area, Peñuela et al. (2013) normalized the depression storage component of the RSCf by the MDS. In this paper we use this dimensionless form of the RSCf to characterize functional connectivity. The point on the RSCf where a sharp increase in area contributing to runoff with increasing relative depression storage can be detected is called the connectivity threshold (CT). This behaviour is typically associated with runoff generating surfaces (Darboux, Davy, et al., 2002; Darboux, Gascuel-Odoux, & Davy, 2002; Peñuela et al., 2015). The CT can be interpreted as a measure of the reactivity of a saturated surface to a rain event. It consists of points CT$_x$ and CT$_y$, corresponding to the ratio depression storage/maximum depression storage (x-axis) and the ratio runoff rate/rain rate (y-axis) respectively. Following Peñuela et al. (2013), we do not consider the point CT$_y$ as it represents a border effect, especially for smaller surfaces such as our field samples S1–S8. As CT$_y$ at point CT$_x = 0$ represents the surface initially connected surface to the outflow boundaries, the RSCf methodology is sensitive to surface sample size and input DTM resolution. The point CT$_x$ contains information on functional connectivity, as it depicts the filled percentage of MDS needed before a rapid increase in surface runoff can be observed.

The RSCf is constructed using the output of the fill-and-spill algorithm FASTR, which is similar to the Antoine et al. (2009) model and the Wang and Liu (2006) filling algorithm described in Section 2.3.1 (Appels et al., 2011). For a detailed description, we refer to Appels et al. (2011).

We propose a new method for finding the CT to standardize the procedure and allow for intercomparison between case studies. As

the CT represents a threshold in the hydrologic connectivity of a surface, we opted for a breakpoint analysis as described in Muggeo (2003). We applied the 'segmented' functionality in R to find two linear regressions and the point where they intersect, the breakpoint, which is interpreted as the CT (Muggeo, 2008). In addition to finding the CT, this method potentially provides extra information on the connectivity dynamics of a surface, in which the two linear regressions describe the connectivity regime in the pre-threshold stage (characterized by filling of depression storage) and the post-threshold stage (characterized by spilling from depression storage).

2.4 | Study design

The goals of this study are: (1) to assess the influence of DTM resolution on estimating surface runoff indicators MDS, RR and CT; and (2) to investigate possible empirical relationships between the surface runoff indicators derived from high (5 cm) and low (50 cm) resolution DTMs. The broader aim is to develop a scaling approach that can be used to estimate surface runoff indicators based on the topography of a surface. By dividing the study site into eight surface samples, this case study is designed to explore the scalability and evaluate within-field variability of the surface runoff indicators. The indicators are calculated for the whole study site, for the separate surface samples S1–S8, and for the average of the surface samples using both the high- and low-resolution DTMs. Comparing the values calculated from the high- and low-resolution DTMs will provide valuable insights in the potential application of lower resolution DTMs in estimating parameters that are influenced by small scale topography. Furthermore, indicator estimates derived from the whole field relative to the sample means will help evaluate the representativeness of surface runoff indicators at different spatial scales.

3 | RESULTS

3.1 | Maximum depression storage

MDS for the selected field samples S1–S8 from our study site (Figure 1) ranges from 0.4 to 2.1 mm (50 cm-DTM) and from 1.2 to 4.0 mm (5 cm-DTM; Figure 4). The MDS values calculated from the 5 cm-DTM (y-axis) are roughly twice as large as the values calculated from the 50 cm-DTM (x-axis).

A linear relationship between the estimated MDS for both DTMs can be derived from the graph (R^2 0.98). This result can be attributed to differences in data collection methods (TLS vs. airborne LiDAR), interpolation procedures or actual changes in microtopography that occurred between both data collection periods. We consider actual changes in topography unlikely, as there has been no change in land use for over a decade, and agricultural activities on the field are kept to a minimum (see Section 2.1). Furthermore, since the linear relationship suggests a systematic difference between the datasets, the most likely explanations are differences in data collection methods or interpolation procedures. Variability in MDS calculated for the field samples S1–S8 is large (SD 0.5 and 0.9 mm for the 50 cm-DTM and 5 cm-DTM respectively) compared to their mean absolute values of approximately 1.0 mm (50 cm-DTM) and 2.1 mm (5 cm-DTM). The lower estimates in S1–S6 as compared to S7 and S8 are likely caused by steeper local slope (S3–S6) and by surface compaction and levelling due to use of heavy machinery on the headland (S1 and S2). MDS values calculated for the full domain of the study site (1.1 mm for the 50 cm-DTM and 2.2 mm for the 5 cm-DTM), indicated by the red circle in Figure 4, fall closely to the fitted linear equation. The difference between the average MDS of all surface samples (blue rhombus) and the full domain MDS (red circle) can be interpreted as a boundary effect, resulting from a greater outflow boundary/spatial domain ratio
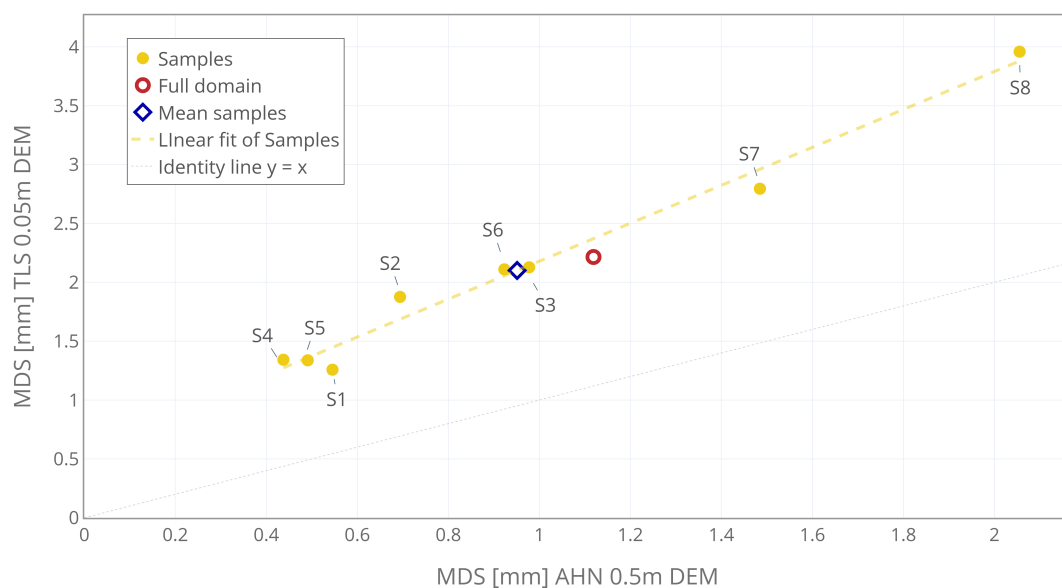
FIGURE 4   MDS in millimetres calculated from the 5 cm-DTM plotted against MDS calculated from the 50 cm-DTM. The points in the graph represent MDS values for the selected field samples S1–S8 (orange), their mean (blue rhombus) and the MDS for the full domain (red circle).

which leads to a higher initially connected surface and therefore a lower number of disconnected surface depressions for the samples. In the filling algorithm used to calculate MDS, only these initially disconnected surface depressions contribute to MDS. As a consequence of the grid cell area/sample area ratio, the boundary effect is more pronounced in the 50 cm-DTM, leading to an 18% difference between mean sample and full domain MDS for the 50 cm-DTM and a 5% difference between mean sample and full domain MDS for the 5 cm-DTM.

3.1.1 | Random roughness

Calculated RR values (Figure 5) in the eight sample plots range from 8.7 to 19.4 mm (50 cm-DTM) and from 11.7 to 22.3 mm (5 cm-DTM). Our results show that estimated RR is consequently higher (Pearson's correlation coefficient = 0.997) for the 5 cm-DTM as compared to the 50 cm-DTM, irrespective of the filter radius used in detrending the surface. Similar to the MDS results, a systematic difference between the outcomes derived from both DTMs can be observed. For the same reasons as mentioned in Section 3.1, the most likely explanations for the observed offset between the 5 cm- and 50 cm-DTM RR are either differences in data collection methods (TLS vs. airborne LiDAR) or the use of inverse distance weighting (IDW) in constructing the 50 cm-DTM, thereby creating a structural and consistent smoothing error of around 2.5 mm.

It is evident that the choice of filter radius strongly influences estimated RR values for both DTMs, leading to RR values roughly twice as large when comparing the lowest (50 cm) and highest (500 cm) filter radii applied in this study. This effect of filter radius can be interpreted as being a consequence of heterogeneity in the sloping surface and the presence of mesotopographic structures which

interfere with the calculations of the filter algorithm. Both aforementioned surface features are present on our case study site (Figure 1). Practically, this means that the larger the filter radius, the bigger the chance that elevation points within the radius deviate from the elevation value at the centre of the filter radius by a larger amount. As the detrended surface used in calculating RR is the result of subtracting the filtered DTM from the original DTM, RR values increase with increasing filter radius. It is important to emphasize that there is no ground truth in a surface analysis based on RR. The choice of a smaller filter radius can highlight roughness at smaller topography scales, such as tussocks and soil aggregates, whereas the choice of a larger filter radius can highlight roughness related to larger surface features, such as rills and gullies generated during land cultivation.

RR values generated from the full domain are consistently higher than the sample average RR values. We attribute this to an underrepresentation of the south-west part of the field site in the surface samples. This more elevated part of the field has higher roughness values, leading to the difference between the sample mean RR and the full domain RR.

3.1.2 | Random roughness derived maximum depression storage

As can be expected from the RR results in the previous section, MDS calculated with the empirical formulas from Table 1 shows a systematic difference between the estimates derived from the two DTMs (Figure 5). MDS derived from the 5 cm-DTM is consistently higher than MDS derived from the 50 cm-DTM for all formulas.

Only the Onstad (1984) formula (filter >1.5 m) is able to accurately estimate the target value, which is defined as the original non-detrended 5 cm-DTM MDS calculated with the Wang and Liu (2006)
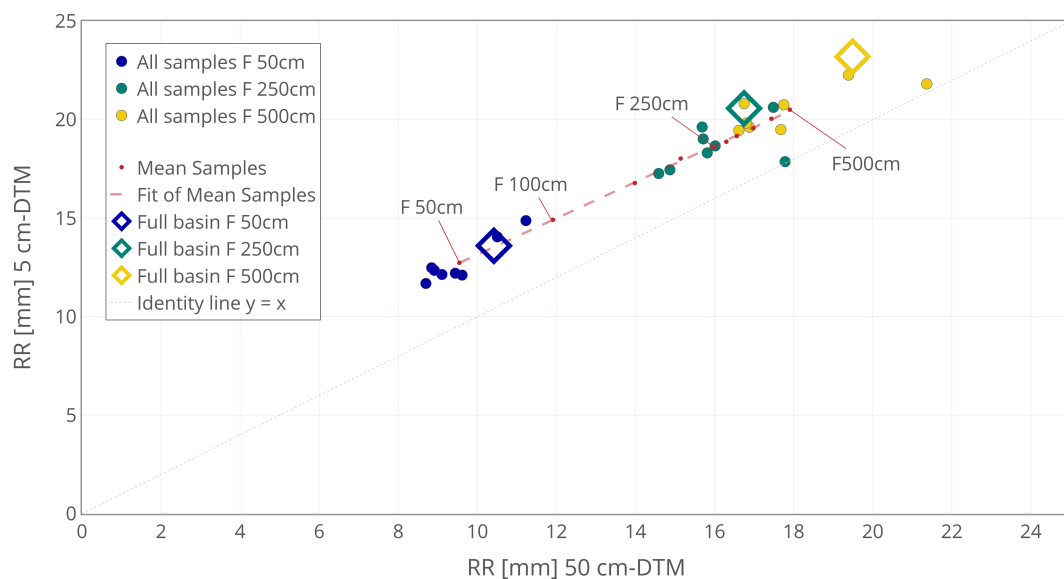
FIGURE 5 RR in millimetres for the 5 cm- and 50 cm-DTMs, plotted for different filter radii used in detrending the surface. The graph shows RR for surface samples S1–S8 (blue, green, and yellow dots), their average (red dots) and for the full domain (rhombi).
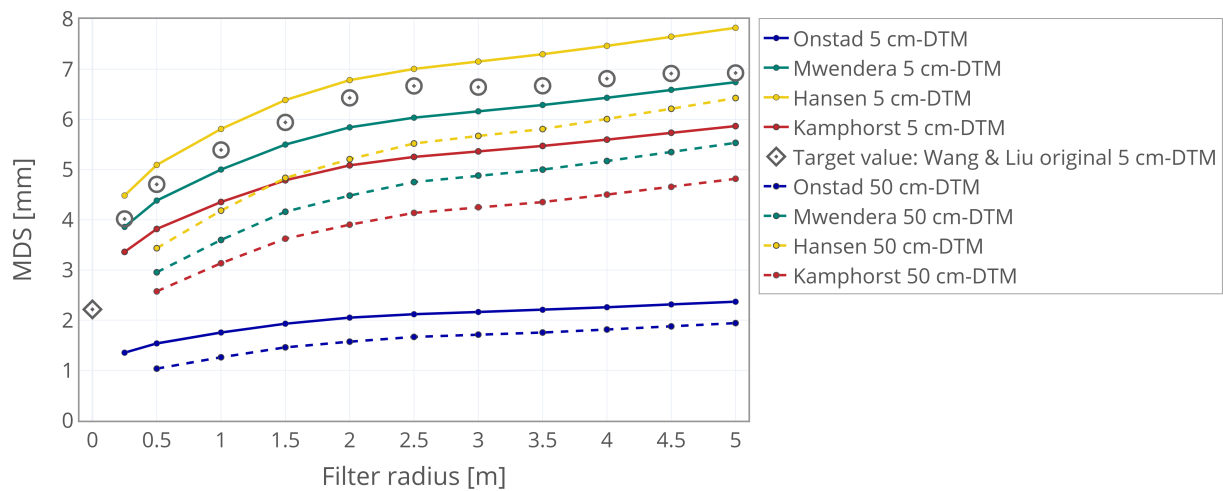
FIGURE 6 MDS in millimetres from empirical formulas (Table 1) for different SAGA Simple Filter radii. RR of the full study domain and a general slope of 1.08% were used in the calculations. For reference, the grey rhombus shows the MDS for the original 5 cm-DTM calculated with the Wang and Liu (2006) filling algorithm, which is regarded the target value. The grey circles show the filling algorithm-based MDS calculated with detrended 5 cm-DTMs as input, highlighting the impact of detrending methods on surface storage properties.

filling algorithm (see Sections 2.3.1 and 3.1). All other formulas using the 5 cm-DTM-derived RR overestimate MDS. The large differences between the outcomes of the empirical formulas indicate that caution should be exercised in the selection of such formulas when used in scientific studies. A large detrending effect is introduced when using a filter algorithm to remove the general slope. In Figure 6, this is evident from the difference between the filling-algorithm based estimates of MDS for the unprocessed (rhombus) and detrended (circles) 5 cm-DTMs (difference of 1.8–4.8 mm). The MDS estimates calculated with the empirical formulas of Mwendera, Hansen and Kamphorst appear to be more closely related to the filling-algorithm based MDS estimates derived from the accompanying detrended DTMs, whereas the Onstad formula predicts MDS more closely to the target value.

From these results, it is evident that RR and the empirical formulas in which RR is used to calculate MDS are strongly affected by the resolution and the construction method of the input DTM, as well as by the detrending methodology used in correcting for slope.

3.2 | Hydrologic connectivity

Relative surface connection functions (RSCf) for the 5 cm- and 50 cm-DTMs show clear differences between the curves obtained from the different input DTMs (Figure 5). The 50 cm-DTM describes the surface as better connected than the 5 cm-DTM, as can be derived from the connectivity thresholds (CT), which are located at the points where the ratio runoff rate/rainfall rate (y-axis) starts to increase substantially. The exact location of CT is arbitrary by design. Peñuela et al. (2013) defined this point at RSCf $dy/dx = 1$. Estimations of this point depend on the window of calculation and are sensitive to local behaviour of the RSCf, meaning that an expert assessment is still required to validate the outcome of the calculations used to determine the CT. Since the CT represents a threshold in surface

connectivity, we opted for a breakpoint analysis to determine its location systematically. The results of the breakpoint analysis are plotted in Figure 7 (circles and rhombi). As argued in the methods Section 2.3.3, point CT_y is sensitive to boundary effects resulting from the size and resolution of the spatial domain, affecting the surface area initially connected to the outflow boundary. Point CT_x is not influenced by this boundary effect.

Point CT_x for the full domain is estimated at $x = 0.20$ for the 50 cm-DTM and at $x = 0.42$ for the 5 cm-DTM. This means that 20% of the 50 cm-DTM depression storage is filled before surface runoff will start to considerably increase, whereas for the 5 cm-DTM this value lies around 42%, which for our study site corresponds to 0.31 mm for the 50 cm-DTM and 0.92 mm for the 5 cm-DTM. For the sample average curves, CT_x values are estimated at 0.49 (50 cm-DTM) and 0.65 (5 cm-DTM), corresponding to 0.76 and 1.42 mm, respectively. This implies that when using the RSCf methodology, the estimation of the runoff response of a saturated surface to a rain event is greatly impacted by the representation of microtopography in the input DTM. It suggests that unconnected microdepressions not captured in the coarser resolution DTM play a role in the connectivity of the study site. The differences between the 5 cm-DTM CT_x estimates of the samples and their means, and the full domain are counterintuitive. The full domain seems better connected than the samples S1–S8. A possible reason is the slightly lower value of MDS calculated for the samples than for the full domain (see Section 3.1), which could alter relative depression filling dynamics. This reveals that the scalability of the RSCf methodology is not straightforward and requires in-depth knowledge of the representability of the surface samples used to explain connectivity at larger scales. The 5 cm-DTM CT_x estimates are consequently higher than their 50 cm-DTM counterparts, indicating that the use of a coarser DTM leads to a more hydrologically connected surface, implying a higher chance of surface runoff.
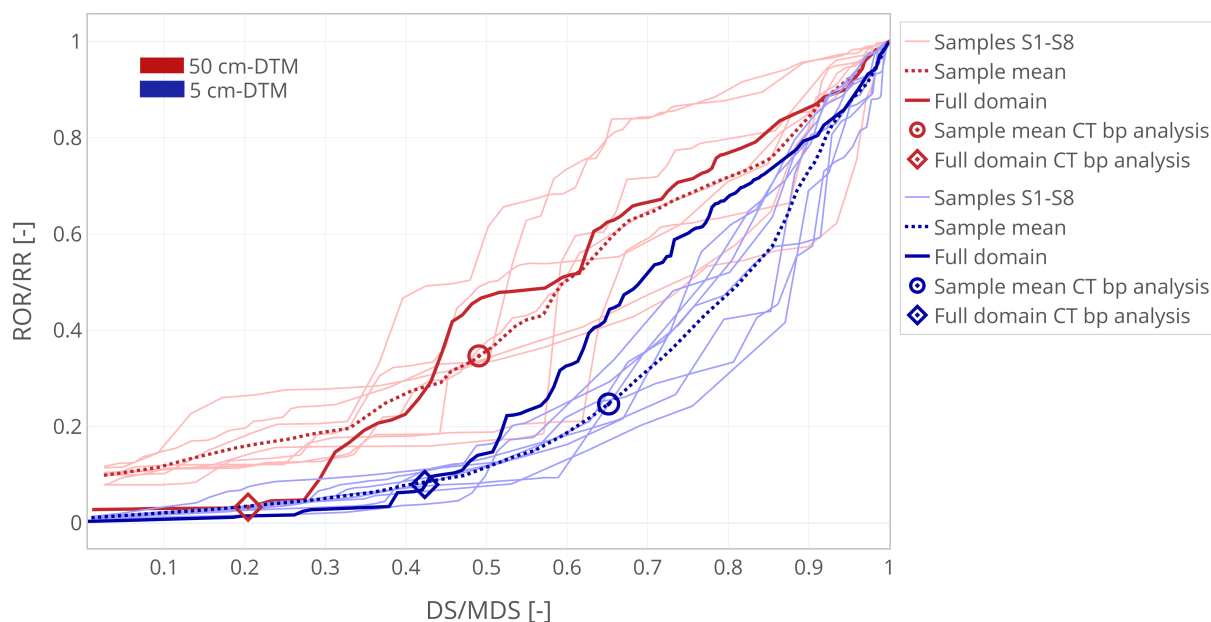
FIGURE 7 Relative Surface Connection Function (RSCf) for the 5 cm-DTM (blue) and 50 cm-DTM (red) with the ratio runoff rate/rain rate (–) on the y-axis and the ratio depression storage/maximum depression storage (–) on the x-axis. Both the full domain (dark lines) and the surface samples S1–S8 (light lines) are plotted, as well as the sample mean (dotted lines). Breakpoint analysis estimates of the connectivity threshold (CT) are also shown for the full domain (rhombi) and the sample means (circles).

All three surface runoff indicators demonstrate a dependency on input DTM resolution. The 50 cm-DTM fails to capture microdepressions and the connections between them, which significantly influence the estimates of MDS, RR and CT. The characteristic features of our study site, tussocks and the spaces between them, necessitate a DTM resolution on the centimetre to decimetre scale for accurate representation. If a lower resolution DTM is used, in our case the 50 cm-DTM, there is a tendency to underestimate MDS and RR while overestimating hydrologic connectivity.

4 | DISCUSSION

In this case study, a 5 cm-DTM and a 50 cm-DTM were used to assess the influence of microtopography on estimating surface runoff indicators maximum depression storage (MDS), random roughness (RR) and the connectivity threshold (CT). Our results show that the surface runoff indicator estimates are sensitive to input data resolution. For our case study site, using the 50 cm-DTM leads to lower estimates of MDS and RR, and to higher estimates of CT compared to the estimates based on the 5 cm-DTM. When integrated into hydrological models, surface runoff indicator estimates based on coarser resolution DTMs could therefore lead to overcompensating with other parameters in calibration procedures, thereby contributing to the well discussed equifinality problem (Beven & Binley, 1992; Kirchner, 2006).

The majority of scientific studies relating DTM resolution to depression storage (Habtezion et al., 2016; Huang & Bradford, 1990; Martin et al., 2008; Yang & Chu, 2013), random roughness (Li

et al., 2020) and functional hydrologic connectivity (Habtezion et al., 2016; Yang & Chu, 2013) agrees with our findings. Notable exceptions can be found in Abedini et al. (2006) and Kamphorst et al. (2000), who found MDS decreasing and unchanged with decreasing DTM resolution respectively. We attribute the results of Abedini et al. (2006) to a border effect resulting from closed boundary conditions in calculating MDS on the west, north and east side of their study domains (areas of 1 m^2). Kamphorst et al. (2000) analysed 221 lab- and agricultural surfaces (areas from 0.2 to 3.5 m^2) and found no significant differences in the calculated MDS for grid spacings from 2 to 40 mm. This work was one of the reasons a 5 cm-DTM was chosen as the 'high' resolution dataset in this study. To the best of our knowledge, this is the first analysis that relates field scale, high resolution measurements to national scale data. We hereby hope to bridge the gap between what is necessary (high-resolution, labour-intensive datasets) and what is publicly available (lower-resolution, national datasets) for DTM-based estimates of surface runoff indicators. A big improvement would be the determination of relevant topography scales for surfaces with similar land use or land cover, defining the grid size needed to capture the storage, roughness and connectivity properties of a surface.

The results show that within-field variation of MDS is large (factor 4) on our study site. Different factors play a role in shaping the surface, including vegetation type and its growth properties, trampling by cattle, grazing frequency, the amount and methods of fertilizer application using heavy machinery, local climate, and the presence of micro- and macro-biota. Most of these shaping factors are defined at the centimetre to decimetre scale. Although these processes are spatially and temporally dynamic in nature and difficult to quantify, the

linear relationship we found between the MDS of the 5 cm- and 50 cm-DTMs (for samples S1–S8) suggest that empirical relationships can be established. The 10 years between the construction of both DTMs can in this light be seen as a shortcoming of this study, but also as an indicator that shaping processes over time do not necessarily impact the geostatistical properties of a surface. This opens the possibility of parameterizing surfaces based on land use or land cover. Repetition of our experiment on similar fields at different points in time and comparing different land uses could contribute to exploring this potential for geostatistical similarity. Since this case study was focussed on evaluating the application of national scale data in estimating surface runoff indicators, we did not include an analysis on the origins of the observed differences between both DTMs. We do acknowledge however, that future research based on our findings would greatly benefit from quantifying the impact of data collection methods and timing, and interpolation procedures. This would help interpreting the meaning of empirical, linear relationships, such as the one we found in this study.

The use of RR requires a slope corrected surface. The correction for slope is often done by subtracting a linear trend plane from the elevation data. This could work well for small sample areas but becomes problematic when considering larger natural landscapes with variation in the sloping surface, as the residuals will become increasingly deviated from the mean. As these residuals determine the RR, this methodology is flawed by design for use on larger surfaces. In this study the SAGA GIS simple filter functionality is used to generate the detrended DTM, but this comes at the expense of representing topographic features by averaging values within a search radius, leading to DTM-smoothing for small search radii or DTM-roughening for large search radii. For the small search radii, this translates to flattening of topography by removing surface features on the decimetre to meter scale. For large search radii, the increasing chance of elevation points deviating from the elevation of the centre grid cell leads to higher residual values, which is translated to a rougher detrended DTM. To date, no methodology has been proposed that is able to account for heterogeneity in the sloping surface in the important pre-processing step of detrending a surface before calculating RR. The detrending method used in this study resulted in a large difference in MDS calculated with the filling algorithm between the detrended and non-detrended 5 cm-DTMs. Across the full range of filter radii used, MDS values were roughly 2–3 times larger for the detrended surfaces compared to the original surface, indicating substantially altered surface characteristics. This stresses the importance of quantifying the effects of the detrending method used in RR-based research.

An in this study unexplored opportunity is the use of raw point clouds instead of interpolated DTM products. Theoretically, these raw data should contain similar geostatistical information across different scales, provided that the analysed surface samples are representative, and that vertical measurement error is of equal magnitude. As RR is calculated as the standard deviation of a for slope corrected surface, it is not dependent on a prepared grid. RR and RR-based empirical formulas used in estimating MDS, are therefore more suited for this approach than filling-algorithm-based MDS and CT, which do require a prepared grid.

Hydrologic connectivity has been identified as a key-concept in hydrology, having the potential to bridge the gap between static surface storage parameters and dynamic (surface) runoff processes (Antoine et al., 2009). In this study, we found that the performance of the RSCf framework, utilizing the CT to quantify hydrologic connectivity, is strongly dependent on the resolution of the input DTM. We also found a scaling issue, following the counterintuitive observation that the full study site of the 5 cm-DTM was more hydrologically connected than the separate samples S1–S8. This raises the question whether this methodology can be applied at small scales to explain connectivity at larger scales. Further research on the scalability of the RSCf methodology is necessary to determine its potential for use in hydrologic modelling.

The hydrological processes governing surface runoff vary with spatial scales and landscape topographic characteristics. In sloping, heterogeneous terrain, macro- and meso-topography will dominate runoff dynamics on saturated soils, while in flat landscapes microtopography takes precedence. Numerous studies on surface runoff have analysed depression storage and hydrologic connectivity based on meter-scale input DTMs (e.g., Barron et al., 2011; Jiang et al., 2023; Wang et al., 2021; Zhu et al., 2013). While the dominance of meso- and macro-topography in these studies justifies the use of meter-scale data, our results show that flat landscapes require higher resolution DTMs for accurate estimates of storage and connectivity properties. Analogue to the broadly accepted terms catchment- and wetland-hydrology, we propose a new sub-discipline: lowland hydrology. This distinction could contribute to frame theoretical insights within the context of flat landscapes, thereby enabling generalizations and upscaling without losing credibility due to the comparison of these insights with research conducted in landscapes dominated by macro- and meso-relief. An example of a lowland-specific opportunity is the construction of tables containing values of MDS, RR and CT, classified by land use and based on repeated high-resolution measurements and empirical relationships with publicly available lower-resolution DTMs. Such empirical tables would also pave the way for addressing the time-restricted nature of DTM-derived parameters, by identifying key topography-shaping moments throughout the season (e.g., tilling, harvesting, etc.) and their impact on surface runoff indicator values.

Our findings reveal a fundamental issue in the way we model and understand the hydrological processes of surface runoff in flat landscapes: If the topographic properties governing surface runoff in saturated conditions (surface storage and hydrologic connectivity) are defined at the centimetre scale, how should we interpret modelling outcomes that utilize coarser scale DTMs? Based on the results of this study, we argue that in flat landscapes, the use of coarser scale DTMs leads to underestimation of MDS and RR, and overestimation of CT. Consequently, there is a need to develop scaling relationships that can quantify these effects in the absence of high resolution DTM data. The observed linear correlation between MDS values derived from high- and lower-resolution DTMs in this study offers a potential method of addressing the loss of information arising from the use of coarser scale DTMs. Further research is needed to evaluate the scalability of RR and CT.

5 | CONCLUSION

Our results show that estimates of surface runoff indicators maximum depression storage (MDS), random roughness (RR) and connectivity threshold (CT) are severely impacted by the spatial resolution of the digital terrain model (DTM) used in the calculations. Filling-algorithm derived MDS values were roughly twice as high for the 5 cm-DTM as compared to the 50 cm-DTM for both the surface samples S1–S8 and the full study site domain. RR of the full study site was consistently estimated to be around 3–4 mm higher when using the 5 cm-DTM as input, independent of the detrending filter radius applied. This amounts to 15%–35% of the absolute values across the full range of RR calculations in this study, that is, RR values for both the input DTMs and for all utilized filter radii in the detrending process (RR range: 10.4–23.7 mm). This translated into consistent differences of MDS calculated with the empirical formulas (Table 1) between the input DTMs. Estimates of point CT_x, the parameter used to quantify functional hydrologic connectivity, were also significantly impacted by the input DTM resolution. Both the CT_x for the sample means (0.65 for the 5 cm-DTM and 0.49 for the 50 cm-DTM) and the CT_x for the full study site domain (0.42 for the 5 cm-DTM and 0.20 for the 50 cm-DTM) showed high dependence on DTM resolution.

A crucial consideration for all research on these surface properties is that the use of interpolated DTM products with insufficient resolution, that is, unable to capture microtopographic surface features, will cause underestimation of MDS and RR, and overestimation of functional hydrologic connectivity. Estimating surface runoff indicators in flat landscapes from commonly available, lower-resolution DTMs will therefore lead to overestimation of surface runoff, necessitating compensatory adjustments with other parameters when integrated into hydrological models. An important step in establishing a better understanding of the relevant topography scales of different surfaces would be the development of a measurement driven knowledge base coupling land use or land cover to the scales at which MDS, RR and hydrologic connectivity are defined. Our outcomes suggest that for MDS, an alternative might be found in the development of empirical formulas that account for the lack of information associated with coarser scale DTMs. MDS results for the surface samples S1–S8 appeared to fit a linear regression between the values of the 5 cm- and 50 cm-DTMs. Such a linear response suggests a possibility to develop an easy way of reverse engineering DTM smoothing caused by interpolation methods. High resolution surface measurements with terrestrial or UAV-LiDAR scanners will contribute to solidifying land use-specific empirical relationships.

Quantifying surface runoff in flat landscapes remains a key challenge in hydrology and water management. Due to the impracticality of direct measurements, our understanding largely hinges on modelling studies. As we found that surface runoff indicators MDS, RR and CT are defined at the centimetre scale, it is imperative for the parameterization of topography to account for this scale-dependency. Explorations such as the one offered in this case study have the potential to reduce parameter ambiguity of surface runoff indicators used in hydrological modelling. As climate change projections indicate an increase in the frequency and intensity of heavy rain events, our research contributes to better understanding its impacts on the hydrological response of surface systems. Our results should be seen as indicative of flat landscapes such as lowlands and river deltas and surfaces where centimetre scale microtopography is relevant.

DATA AVAILABILITY STATEMENT

The data that support the findings of this study are available from the corresponding author upon reasonable request.

ORCID

Peter Schaap https://orcid.org/0000-0003-2358-542X
Ype van der Velde https://orcid.org/0000-0002-2183-2573
Perry de Louw https://orcid.org/0009-0008-9680-4412
Harm Bartholomeus https://orcid.org/0000-0002-1905-7678

REFERENCES

Abd Elbasit, M. A., Abu-Zreig, M. M., Ojha, C. S. P., Yasuda, H., & Gang, L. (2020). Estimation of surface depression storage capacity from random roughness and slope. *Water SA*, *46*(3 July), 404–409. https://doi.org/10.17159/wsa/2020.v46.i3.8650

Abedini, M. J., Dickinson, W. T., & Rudra, R. P. (2006). On depressional storages: The effect of DEM spatial resolution. *Journal of Hydrology*, *318*(1–4), 138–150. https://doi.org/10.1016/j.jhydrol.2005.06.010

Amoah, J. K. O., Amatya, D. M., & Nnaji, S. (2013). Quantifying watershed surface depression storage: Determination and application in a hydrologic model. *Hydrological Processes*, *27*(17), 2401–2413. https://doi.org/10.1002/hyp.9364

Antoine, M., Javaux, M., & Bielders, C. (2009). What indicators can capture runoff-relevant connectivity properties of the micro-topography at the plot scale? *Advances in Water Resources*, *32*(8), 1297–1310. https://doi.org/10.1016/j.advwatres.2009.05.006

Appels, W. M., Bogaart, P. W., & van der Zee, S. E. A. T. M. (2011). Influence of spatial variations of microtopography and infiltration on surface runoff and field scale hydrological connectivity. *Advances in Water Resources*, *34*(2), 303–313. https://doi.org/10.1016/j.advwatres.2010.12.003

Appels, W. M., Bogaart, P. W., & van der Zee, S. E. A. T. M. (2016). Surface runoff in flat terrain: How field topography and runoff generating processes control hydrological connectivity. *Journal of Hydrology*, *534*, 493–504. https://doi.org/10.1016/j.jhydrol.2016.01.021

Aquanty. (2015). *HydroGeoSphere theory manual* (No. 2531) (p. 114). Aquanty Inc. https://aquanty-artifacts-public.s3.amazonaws.com/hgs/hydrosphere_theory.pdf

Barneveld, R. J., van der Zee, S. E. A. T. M., & Stolte, J. (2019). Quantifying the dynamics of microtopography during a snowmelt event. *Earth Surface Processes and Landforms*, *44*(13), 2544–2556. https://doi.org/10.1002/esp.4678

Barron, O. V., Pollock, D., & Dawes, W. (2011). Evaluation of catchment contributing areas and storm runoff in flat terrain subject to urbanisation. *Hydrology and Earth System Sciences*, *15*(2), 547–559. https://doi.org/10.5194/hess-15-547-2011

Beven, K. (1989). Changing ideas in hydrology—The case of physically-based models. *Journal of Hydrology*, 105(1–2), 157–172. https://doi.org/10.1016/0022-1694(89)90101-7

Beven, K., & Binley, A. (1992). The future of distributed models: Model calibration and uncertainty prediction. *Hydrological Processes*, 6(3), 279–298. https://doi.org/10.1002/hyp.3360060305

Beven, K. J., & Kirkby, M. J. (1979). A physically based, variable contributing area model of basin hydrology/Un modèle à base physique de zone d'appel variable de l'hydrologie du bassin versant. *Hydrological Sciences Bulletin*, 24(1), 43–69. https://doi.org/10.1080/02626667909491834

Burwell, R. E., Timmons, D. R., & Holt, R. F. (1975). Nutrient transport in surface runoff as influenced by soil cover and seasonal periods. *Soil Science Society of America Journal*, 39(3), 523–528. https://doi.org/10.2136/sssaj1975.03615995003900030040x

Cavalli, M., & Marchi, L. (2008). Characterisation of the surface morphology of an alpine alluvial fan using airborne LiDAR. *Natural Hazards and Earth System Sciences*, 8(2), 323–333. https://doi.org/10.5194/nhess-8-323-2008

Chrétien, F., Giroux, I., Thériault, G., Gagnon, P., & Corriveau, J. (2017). Surface runoff and subsurface tile drain losses of neonicotinoids and companion herbicides at edge-of-field. *Environmental Pollution*, 224, 255–264. https://doi.org/10.1016/j.envpol.2017.02.002

Chu, X., Yang, J., & Chi, Y. (2012). Quantification of soil random roughness and surface depression storage: Methods, applicability, and limitations. *Transactions of the ASABE*, 55(5), 1699–1710. https://doi.org/10.13031/2013.42361

Chu, X., Zhang, J., Yang, J., & Chi, Y. (2010). Quantitative evaluation of the relationship between grid spacing of DEMs and surface depression storage. In *World environmental and water resources congress 2010: Challenges of change* (pp. 4447–4457).

Coumou, D., & Rahmstorf, S. (2012). A decade of weather extremes. *Nature Climate Change*, 2(7), 491–496. https://doi.org/10.1038/nclimate1452

Coyne, M. S., Gilfillen, R. A., Rhodes, R. W., & Blevins, R. L. (1995). Soil and fecal coliform trapping by grass filter strips during simulated rain. *Journal of Soil and Water Conservation*, 50(4), 405–408.

Currence, H. D., & Lovely, W. G. (1970). The analysis of soil surface roughness. *Transactions of the ASAE*, 13(6), 710–714.

Cremers, N. H. D. T., Van Dijk, P. M., De Roo, A. P. J., & Verzandvoort, M. A. (1996). Spatial and temporal variability of soil surface roughness and the application in hydrological and soil erosion modelling. *Hydrological Processes*, 10(8), 1035–1047. https://doi.org/10.1002/(SICI)1099-1085(199608)10:8<1035::AID-HYP409>3.0.CO;2-%23

Dąbrowska, J., Dąbek, P., & Lejcuś, I. (2018). Identifying surface runoff pathways for cost-effective mitigation of pollutant inputs to drinking water reservoir. *Water*, 10(10), 1300. https://doi.org/10.3390/w10101300

Darboux, F., Davy, P., Gascuel-Odoux, C., & Huang, C. (2002). Evolution of soil surface roughness and flowpath connectivity in overland flow experiments. *Catena*, 46(2–3), 125–139. https://doi.org/10.1016/S0341-8162(01)00162-X

Darboux, F., Gascuel-Odoux, C., & Davy, P. (2002). Effects of surface water storage by soil roughness on overland-flow generation. *Earth Surface Processes and Landforms*, 27(3), 223–233. https://doi.org/10.1002/esp.313

De Louw, P., Kuijper, M., Drost, R., Hendriks, D., Rozemeijer, J., & Stuyt, L. (2015). *Veldonderzoek oppervlakkige afstroming en regelbare drainage in het kader van DROP*.

De Roo, A. P. J., Offermans, R. J. E., & Cremers, N. H. D. T. (1996). LISEM: A single-event, physically based hydrological and soil erosion model for drainage basins. I: Theory, input and output. *Hydrological Processes*, 10(8), 1119–1126. https://doi.org/10.1002/(SICI)1099-1085(199608)10:8<1119::AID-HYP416>3.0.CO;2-V

de Vries, W., Schulte-Uebbing, L., Kros, H., Voogd, J. C., & Louwagie, G. (2021). Spatially explicit boundaries for agricultural nitrogen inputs in the European Union to meet air and water quality targets. *Science of the Total Environment*, 786, 147283. https://doi.org/10.1016/j.scitotenv.2021.147283

Desmet, P. J. J. (1997). Effects of interpolation errors on the analysis of DEMs. *Earth Surface Processes and Landforms*, 22(6), 563–580. https://doi.org/10.1002/(SICI)1096-9837(199706)22:6<563::AID-ESP713>3.0.CO;2-3

DHI. (2023). *MIKE SHE user guide and reference manual*.

Dolph, C. L., Boardman, E., Danesh-Yazdi, M., Finlay, J. C., Hansen, A. T., Baker, A. C., & Dalzell, B. (2019). Phosphorus transport in intensively managed watersheds. *Water Resources Research*, 55(11), 9148–9172. https://doi.org/10.1029/2018WR024009

Dudgeon, D. (2019). Multiple threats imperil freshwater biodiversity in the Anthropocene. *Current Biology*, 29(19), R960–R967. https://doi.org/10.1016/j.cub.2019.08.002

Dunne, T., Zhang, W., & Aubry, B. F. (1991). Effects of rainfall, vegetation, and microtopography on infiltration and runoff. *Water Resources Research*, 27(9), 2271–2285. https://doi.org/10.1029/91WR01585

EC. (2000). Directive 2000/60/EC of the European parliament and of the council of 23 October 2000; establishing a framework for community action in the field of water policy. *Official Journal of the European Communities*, 327(1), 1–71.

Fan, L., & Atkinson, P. M. (2018). A new multi-resolution based method for estimating local surface roughness from point clouds. *ISPRS Journal of Photogrammetry and Remote Sensing*, 144, 369–378. https://doi.org/10.1016/j.isprsjprs.2018.08.003

Frei, S., & Fleckenstein, J. H. (2014). Representing effects of micro-topography on runoff generation and sub-surface flow patterns by using superficial rill/depression storage height variations. *Environmental Modelling & Software*, 52, 5–18. https://doi.org/10.1016/j.envsoft.2013.10.007

Frei, S., Lischeid, G., & Fleckenstein, J. H. (2010). Effects of micro-topography on surface–subsurface exchange and runoff generation in a virtual riparian wetland—A modeling study. *Advances in Water Resources*, 33(11), 1388–1401. https://doi.org/10.1016/j.advwatres.2010.07.006

Gilliom, R. J. (2007). Pesticides in U.S. streams and groundwater. *Environmental Science & Technology*, 41(10), 3408–3414. https://doi.org/10.1021/es072531u

Gomi, T., Sidle, R. C., Miyata, S., Kosugi, K., & Onda, Y. (2008). Dynamic runoff connectivity of overland flow on steep forested hillslopes: Scale effects and runoff transfer. *Water Resources Research*, 44(8), 1–16. https://doi.org/10.1029/2007WR005894

Habtezion, N., Tahmasebi Nasab, M., & Chu, X. (2016). How does DEM resolution affect microtopographic characteristics, hydrologic connectivity, and modelling of hydrologic processes? *Hydrological Processes*, 30(25), 4870–4892. https://doi.org/10.1002/hyp.10967

Hansen, B., Schjønning, P., & Sibbesen, E. (1999). Roughness indices for estimation of depression storage capacity of tilled soil surfaces. *Soil and Tillage Research*, 52(1–2), 103–111. https://doi.org/10.1016/S0167-1987(99)00061-6

Harpold, A. A., Marshall, J. A., Lyon, S. W., Barnhart, T. B., Fisher, B. A., Donovan, M., Brubaker, K. M., Crosby, C. J., Glenn, N. F., Glennie, C. L., Kirchner, P. B., Lam, N., Mankoff, K. D., McCreight, J. L., Molotch, N. P., Musselman, K. N., Pelletier, J., Russo, T., Sangireddy, H., … West, N. (2015). Laser vision: Lidar as a transformative tool to advance critical zone science. *Hydrology and Earth System Sciences*, 19(6), 2881–2897. https://doi.org/10.5194/hess-19-2881-2015

Haygarth, P. M., Wood, F. L., Heathwaite, A. L., & Butler, P. J. (2005). Phosphorus dynamics observed through increasing scales in a nested headwater-to-river channel study. *Science of the Total Environment*, 344(1), 83–106. https://doi.org/10.1016/j.scitotenv.2005.02.007

Heathwaite, A. L., & Dils, R. M. (2000). Characterising phosphorus loss in surface and subsurface hydrological pathways. *Science of the Total Environment*, 251–252, 523–538. https://doi.org/10.1016/S0048-9697(00)00393-4

Huang, C., & Bradford, J. M. (1990). Depressional storage for Markov-Gaussian surfaces. *Water Resources Research*, 26(9), 2235–2242. https://doi.org/10.1029/WR026i009p02235

Jan, A., Coon, E. T., Graham, J. D., & Painter, S. L. (2018). A subgrid approach for modeling microtopography effects on overland flow. *Water Resources Research*, 54(9), 6153–6167. https://doi.org/10.1029/2017wr021898

Jensen, C. K., McGuire, K. J., & Prince, P. S. (2017). Headwater stream length dynamics across four physiographic provinces of the Appalachian Highlands. *Hydrological Processes*, 31(19), 3350–3363. https://doi.org/10.1002/hyp.11259

Jiang, A. L., Hsu, K., Sanders, B. F., & Sorooshian, S. (2023). Topographic hydro-conditioning to resolve surface depression storage and ponding in a fully distributed hydrologic model. *Advances in Water Resources*, 176(November 2022), 104449. https://doi.org/10.1016/j.advwatres.2023.104449

Joel, A., Messing, I., Seguel, O., & Casanova, M. (2002). Measurement of surface water runoff from plots of two different sizes. *Hydrological Processes*, 16(7), 1467–1478. https://doi.org/10.1002/hyp.356

Kamphorst, E. C., Jetten, V., Guérif, J., Pitk änen, J., Iversen, B. V., Douglas, J. T., & Paz, A. (2000). Predicting depressional storage from soil surface roughness. *Soil Science Society of America Journal*, 64(5), 1749–1758. https://doi.org/10.2136/sssaj2000.6451749x

Kirchner, J. W. (2006). Getting the right answers for the right reasons: Linking measurements, analyses, and models to advance the science of hydrology. *Water Resources Research*, 42(3), 1–5. https://doi.org/10.1029/2005WR004362

Kool, M., Kosters, H., Griffioen, J., Groothuijse, F. A. G., & Buitenkamp, M. (2023). *Wie Aa zegt...; Aanbevelingen voor duurzame verbetering van de waterkwaliteit van de Drentsche Aa ten behoeve van de openbare drinkwatervoorziening*.

Kopecký, M., Macek, M., & Wild, J. (2021). Topographic wetness index calculation guidelines based on measured soil moisture and plant species composition. *Science of the Total Environment*, 757(November), 143785. https://doi.org/10.1016/j.scitotenv.2020.143785

Kroes, J. G., Van Dam, J. C., Bartholomeus, R. P., Groenendijk, P., Heinen, M., Hendriks, R. F. A., Mulder, H. M., Supit, I., & Van Walsum, P. E. V. (2017). *SWAP version 4* (p. 248). Wageningen Environmental Research.

Leip, A., Billen, G., Garnier, J., Grizzetti, B., Lassaletta, L., Reis, S., Simpson, D., Sutton, M. A., de Vries, W., Weiss, F., & Westhoek, H. (2015). Impacts of European livestock production: Nitrogen, sulphur, phosphorus and greenhouse gas emissions, land-use, water eutrophication and biodiversity. *Environmental Research Letters*, 10(11), 115004. https://doi.org/10.1088/1748-9326/10/11/115004

Li, L., Nearing, M. A., Nichols, M. H., Polyakov, V. O., Phillip Guertin, D., & Cavanaugh, M. L. (2020). The effects of DEM interpolation on quantifying soil surface roughness using terrestrial LiDAR. *Soil and Tillage Research*, 198(January), 104520. https://doi.org/10.1016/j.still.2019.104520

Markstrom, S. L., Regan, R. S., Hay, L. E., Viger, R. J., Webb, R. M., Payn, R. A., & LaFontaine, J. H. (2015). PRMS-IV, the precipitation-runoff modeling system, version 4. *US Geological Survey Techniques and Methods*, 6, B7.

Martin, Y., Valeo, C., & Tait, M. (2008). Centimetre-scale digital representations of terrain and impacts on depression storage and runoff. *Catena*, 75(2), 223–233. https://doi.org/10.1016/j.catena.2008.07.005

Massop, H. T. L., Van Bakel, P. J. T., & De Louw, P. G. B. (2017). *Maatgevende afvoer en maaiveldafvoer in waterschap Vechtstromen*. https://doi.org/10.18174/425042

Moriasi, D. N., Rossi, C. G., Arnold, J. G., & Tomer, M. D. (2012). Evaluating hydrology of the soil and water assessment tool (SWAT) with new tile drain equations. *Journal of Soil and Water Conservation*, 67(6), 513–524. https://doi.org/10.2489/jswc.67.6.513

Moudrý, V., Klápště, P., Fogl, M., Gdulová, K., Barták, V., & Urban, R. (2020). Assessment of LiDAR ground filtering algorithms for determining ground surface of non-natural terrain overgrown with forest and steppe vegetation. *Measurement*, 150, 107047. https://doi.org/10.1016/j.measurement.2019.107047

Muggeo, V. M. R. (2003). Estimating regression models with unknown break-points. *Statistics in Medicine*, 22(19), 3055–3071. https://doi.org/10.1002/sim.1545

Muggeo, V. M. R. (2008). Segmented: An R package to fit regression models with broken-line relationships. *R News*, 8(1), 20–25. https://cran.r-project.org/doc/Rnews/

Mwendera, E. J., & Feyen, J. (1992). Estimation of depression storage and Manning's resistance coefficient from random roughness measurements. *Geoderma*, 52(3–4), 235–250. https://doi.org/10.1016/0016-7061(92)90039-A

Neitsch, S. L., Arnold, J. G., Kiniry, J. R., & Williams, J. R. (2011). *Soil and water assessment tool theoretical documentation version 2009*. Texas Water Resources Institute.

Niittynen, P., Heikkinen, R. K., & Luoto, M. (2018). Snow cover is a neglected driver of Arctic biodiversity loss. *Nature Climate Change*, 8(11), 997–1001. https://doi.org/10.1038/s41558-018-0311-x

Onstad, C. A. (1984). Depressional storage on tilled soil surfaces. *Transactions of the ASAE*, 27(3), 729–732.

Panday, S., & Huyakorn, P. S. (2004). A fully coupled physically-based spatially-distributed model for evaluating surface/subsurface flow. *Advances in Water Resources*, 27(4), 361–382. https://doi.org/10.1016/j.advwatres.2004.02.016

Peñuela, A., Javaux, M., & Bielders, C. L. (2013). Scale effect on overland flow connectivity at the plot scale. *Hydrology and Earth System Sciences*, 17(1), 87–101. https://doi.org/10.5194/hess-17-87-2013

Peñuela, A., Javaux, M., & Bielders, C. L. (2015). How do slope and surface roughness affect plot-scale overland flow connectivity? *Journal of Hydrology*, 528, 192–205. https://doi.org/10.1016/j.jhydrol.2015.06.031

Peyton, D. P., Healy, M. G., Fleming, G. T. A., Grant, J., Wall, D., Morrison, L., Cormican, M., & Fenton, O. (2016). Nutrient, metal and microbial loss in surface runoff following treated sludge and dairy cattle slurry application to an Irish grassland soil. *Science of the Total Environment*, 541, 218–229. https://doi.org/10.1016/j.scitotenv.2015.09.053

Rakonjac, N., van der Zee, S. E. A. T. M., Wipfler, L., Roex, E., & Kros, H. (2022). Emission estimation and prioritization of veterinary pharmaceuticals in manure slurries applied to soil. *Science of the Total Environment*, 815, 152938. https://doi.org/10.1016/j.scitotenv.2022.152938

Rakonjac, N., van der Zee, S. E. A. T. M., Wipfler, L., Roex, E., Urbina, C. A. F., Borgers, L. H., & Ritsema, C. J. (2023). An analytical framework on the leaching potential of veterinary pharmaceuticals: A case study for The Netherlands. *Science of the Total Environment*, 859(November 2022), 160310. https://doi.org/10.1016/j.scitotenv.2022.160310

Sharpley, A. N., Chapra, S. C., Wedepohl, R., Sims, I. T., Daniel, T. C., & Reddy, K. R. (1994). Managing agricultural phosphorus for protection of surface waters: Issues and options. *Journal of Environmental Quality*, 23, 437–451.

Smith, D. R., King, K. W., Johnson, L., Francesconi, W., Richards, P., Baker, D., & Sharpley, A. N. (2015). Surface runoff and tile drainage transport of phosphorus in the midwestern United States. *Journal of Environmental Quality*, 44, 495–502. https://doi.org/10.2134/jeq2014.04.0176

Smith, K. A., Jackson, D. R., & Pepper, T. J. (2001). Nutrient losses by surface run-off following the application of organic manures to arable land. 1. Nitrogen. *Environmental Pollution*, 112(1), 41–51. https://doi.org/10.1016/S0269-7491(00)00097-X

Soultani, M., Tan, C. S., Gaynor, J. D., Neveu, R., & Drury, C. F. (1993). Measuring and sampling surface runoff and subsurface drain outflow volume. *Applied Engineering in Agriculture*, *9*(5), 447–450.

Telling, J., Lyda, A., Hartzell, P., & Glennie, C. (2017). Review of earth science research using terrestrial laser scanning. *Earth-Science Reviews*, *169*(March), 35–68. https://doi.org/10.1016/j.earscirev.2017.04.007

Thomas, I. A., Jordan, P., Shine, O., Fenton, O., Mellander, P.-E., Dunlop, P., & Murphy, P. N. C. (2017). Defining optimal DEM resolutions and point densities for modelling hydrologically sensitive areas in agricultural catchments dominated by microtopography. *International Journal of Applied Earth Observation and Geoinformation*, *54*, 38–52. https://doi.org/10.1016/j.jag.2016.08.012

Trevisani, S., Cavalli, M., & Marchi, L. (2012). Surface texture analysis of a high-resolution DTM: Interpreting an alpine basin. *Geomorphology*, *161–162*, 26–39. https://doi.org/10.1016/j.geomorph.2012.03.031

van der Velde, Y., Rozemeijer, J. C., de Rooij, G. H., van Geer, F. C., & Broers, H. P. (2010). Field-scale measurements for separation of catchment discharge into flow route contributions. *Vadose Zone Journal*, *9*(1), 25. https://doi.org/10.2136/vzj2008.0141

Wang, L., & Liu, H. (2006). An efficient method for identifying and filling surface depressions in digital elevation models for hydrologic analysis and modelling. *International Journal of Geographical Information Science*, *20*(2), 193–213. https://doi.org/10.1080/13658810500433453

Wang, N., Chu, X., & Zhang, X. (2021). Functionalities of surface depressions in runoff routing and hydrologic connectivity modeling. *Journal of Hydrology*, *593*(November 2020), 125870. https://doi.org/10.1016/j.jhydrol.2020.125870

Woolhiser, D. A. (1996). Search for physically based runoff model—A hydrologic El Dorado? *Journal of Hydraulic Engineering*, *122*(3), 122–129. https://doi.org/10.1061/(asce)0733-9429(1996)122:3(122)

Worm, B., De Louw, P., Van Bakel, J., & Massop, H. (2019). Maaiveldafvoer: Verkennend onderzoek naar een onderbelicht hydrologisch verschijnsel. H_2O (pp. 32–35).

Wurtsbaugh, W. A., Paerl, H. W., & Dodds, W. K. (2019). Nutrients, eutrophication and harmful algal blooms along the freshwater to marine continuum. *Wiley Interdisciplinary Reviews: Water*, *6*(5), 1–27. https://doi.org/10.1002/wat2.1373

Yang, J., & Chu, X. (2013). Effects of DEM resolution on surface depression properties and hydrologic connectivity. *Journal of Hydrologic Engineering*, *18*(9), 1157–1169. https://doi.org/10.1061/(ASCE)HE.1943-5584.0000731

Zhang, W., & Cundy, T. W. (1989). Modeling of two-dimensional overland flow. *Water Resources Research*, *25*(9), 2019–2035. https://doi.org/10.1029/WR025i009p02019

Zhu, D., Ren, Q., Xuan, Y., Chen, Y., & Cluckie, I. D. (2013). An effective depression filling algorithm for DEM-based 2-D surface flow modelling. *Hydrology and Earth System Sciences*, *17*(2), 495–505. https://doi.org/10.5194/hess-17-495-2013